# Simulation of potential impact of air pollution from the proposed coal mining sites in Mui Basin, Kitui County

**Muthama N. J. [1,a]\*, Kaume C. M. [1,b], Mutai B. K.[1,c] and Ng'ang'a J.K.[1,d]**

[1]*Department of Meteorology, University of Nairobi, P.O Box 30197-00100, Nairobi, Kenya*

[a]*jmuthama@uonbi.ac.ke\*, [b]kaumecm@gmail.com,  [c]berth@uonbi.ac.ke, and [d]jknganga@uonbi.ac.ke*

| ARTICLE INFO | ABSTRACT |
|---|---|
| | The potential for air pollutants transport, dispersion patterns and impacts within and around the Mui basin, Kitui County is simulated. The spatial-temporal distribution of air pollutants from the proposed coal mines was investigated using Hybrid Single Particle Lagrangian Integrated Trajectories (HYSPLIT) and dispersion analyses. The spatial distribution of wind patterns was investigated using wind rose to explain the observed air pollution distribution. The analysis was carried out for the dry and wet seasons of the study area namely: December, January, February (DJF), March, April, May (MAM), June, July, August (JJA) and September, October, November (SON) seasons. From the analysis, the season during which the exposure levels would pose much health threat was established based on frequency of winds blowing in certain direction and speed. By spatial analysis of the proximity of proposed mines and direction of dominant winds, areas most prone to pollution were delineated. The results showed that winds over the area were generally low and southerly. The residents to the northern and northwestern sectors would be at most at risk should the mining commence. Due to low wind speeds during January and the onset of JJA season, residents and workers at the mine would be affected adversely. The results may contribute to the design of effective control strategies to reduce impact of emitted pollutants. |

## 1. Introduction

The Government of Kenya through the Ministry of Energy (MoE) has been conducting exploration since 1999 for coal in the Mui Basin, Kitui County. The basin covers an area of 500 Km$^2$ and is situated about 180 Km North East of Nairobi. So far, seventy-one (71) exploration and appraisal wells have been drilled by the MoE. Appraisal drilling has been concentrated in block C where fifty-six (56) wells were drilled to depths ranging from 75 to 445 meters and coal seams encountered in thirty-two (32) of the wells [1].

Coal samples have been tested for calorific value, carbon content, ash content, moisture content, sulphur, iron and volatile matter content. The laboratory results indicated that Mui coal ranks from peat through lignite and sub-bituminous to bituminous in grade. The discovered coal deposit in Mui basin has been tested and analyzed by the Ministry of Energy which showed that it contained sulphur (2.4%), volatile matter (30%), and ash content (30%) which could have negative air pollution implications [2] and thus health impact to the people [3].

It is, however, noted that economic utilization of coal resources needs an understanding of the effects of coal related pollutant on life and the role of meteorological factors in driving those pollutants. Coal mining operations give rise to air pollution in the form of coal or rock dust and gaseous pollutant. Loading/offloading and transportation of coal, bad condition of roads and open burning of coal are largely responsible for air particulate and gaseous pollutants.

Airborne particulate matter, which is composed of a broad class of chemically and physically diverse substances are variable in size, chemical composition, formation, origin and concentration, and is variable across space and time. Health effects associated with particulate matter (PM) are linked to respiratory, cardiovascular problems and premature mortality [3]. The particulates may include a broad range of chemical species, ranging from metals to organic and inorganic compounds [4]. The airborne particulates and related trace metals have been linked with both acute and chronic adverse health effects which mostly include respiratory diseases, lung cancer, heart diseases and damage to other organs [5-7].

It has been noted that every coal related pollutant e.g. heavy metals like lead, chromium and suspended solids like ashes has its own effect to life and hence concerted efforts should be put to reduce their release [8]. Heavy metals comprise the total dissolved solids. They include arsenic, Barium, Cadmium, Chromium, Lead, Mercury, Selenium and Silver. Even though, they have other sources, coal burning release substantial amount of it and each has its own effect. For instance, inorganic arsenic, which contains carcinogens, can cause cancer of skin, lungs, liver and bladder. Lower level exposure can cause nausea and vomiting, decreased production of red and white blood cells, abnormal heart rhythm, d. Barium on short term exposure can cause vomiting, abdominal cramps, diarrhoea, difficulties in breathing, increased or decreased blood pressure, numbness around the face and muscle weakness while large amount can cause, high blood pressure, changes in heart rhythm or paralysis and possibly death. Oxides of nitrogen ($NO_X$) are by-products of fossil fuel combustion from automobiles and coal-fired power plants, among many other sources. Oxides of nitrogen react with chemicals in the atmosphere to create pollution products such as ozone (smog), nitrous oxide ($N_2O$), and nitrogen dioxide ($NO_2$). $NO_2$ and ozone are pollutants of particular concern.

Global climate change is caused by the accumulation of greenhouse gases in the Earth's atmosphere. Two of the major greenhouse gases contributing to climate change are products of coal combustion: carbon dioxide ($CO_2$) and nitrous oxide ($N_2O$). As the concentrations of these gases in the atmosphere increase, the average global temperature slowly increases, setting in motion a host of consequences that further promote climate change such as melting of polar ice and thawing of the arctic permafrost.

The need for improving access to energy in sub-Saharan Africa is of paramount importance as it offers significant opportunity for achieving sustainable development goals as envisaged in the millennium development goals agenda [9-10]. Kenya through the Ministry of Energy endeavors to secure affordable, reliable, clean and dependable power for provision of essential services such as lighting, heating, cooking, mobility and communication as well as driving industrial growth [11]. This is fundamental to economic stability and development as interruption of energy supplies, for example power rationing between June and November 2006, can cause major financial losses and create economic havoc [12]. According to [12], power outages in Kenya were due to immense pressure on existing power sources like hydropower, geothermal and thermal and high costs of importing additional power from neighboring Uganda, considering a total effective source utilization of 96% of the installed sources.

Though hydro-electric power, a renewable energy source, tops the list of energy sources in Kenya with 646.1 MW of the effective total output [13-14], it is not reliable due to its dependence on weather patterns and may also be affected by environmental degradation. For example, during droughts, power rationing is occasioned by the reduction of water levels in these dams. According to [15], power step-up in such production periods is sourced from independent power producers who use geothermal generation, which is equally expensive. Geothermal power production on the other hand, though constant, is not feasible to step up at a short notice in addition to its high cost of equipment and in technology [14].

This study sought to simulate the potential air pollution transport, dispersion and impacts within and around the proposed sites and contributes to the design of effective control strategies to reduce impact of the emitted harmful air pollutants.

## 2. Data and methods
In this section the area of study, data and methods used in the study are elaborated separately in the following sub-sections.

### 2.1 Area of study
Mui basin lies at approximately latitude 1.366$^o$ South and 38.016$^o$ East and sub-divided into Zombe, Kabati, Itiko, Mutitu, Yoonye, Kateiko, Isekele and Karunga. However, mining activities will be concentrated in Kateiko and Yoonye. To ease exploration logistics, the MoE categorized the basin into four blocks designated as Block A(Zombe-Kabati), block B(Mutitu-Itiko), Block C(Kateiko-Yoonye) and Block D (Karunga-Isekele) measuring 121.5 Km$^2$, 117.5 Km$^2$, 131.5 Km$^2$ and 120 Km$^2$ respectively. The area has rainfall in two distinct seasons (MAM and OND). The month of June to September is usually dry with almost no rains except the month of July, which experiences cool and moist easterlies due to equator-ward extension of Mascarene high pressure ridge with drizzle as the main form of precipitation. Winds in the area are light throughout the year having a maximum of 3.2 ms$^{-1}$ in October and 2.2 ms$^{-1}$ in April. There are occasional dust storms in the entire basin especially on bare land characterized by strong winds mostly in August and September as was averaged over Mui area in 2009 [16].
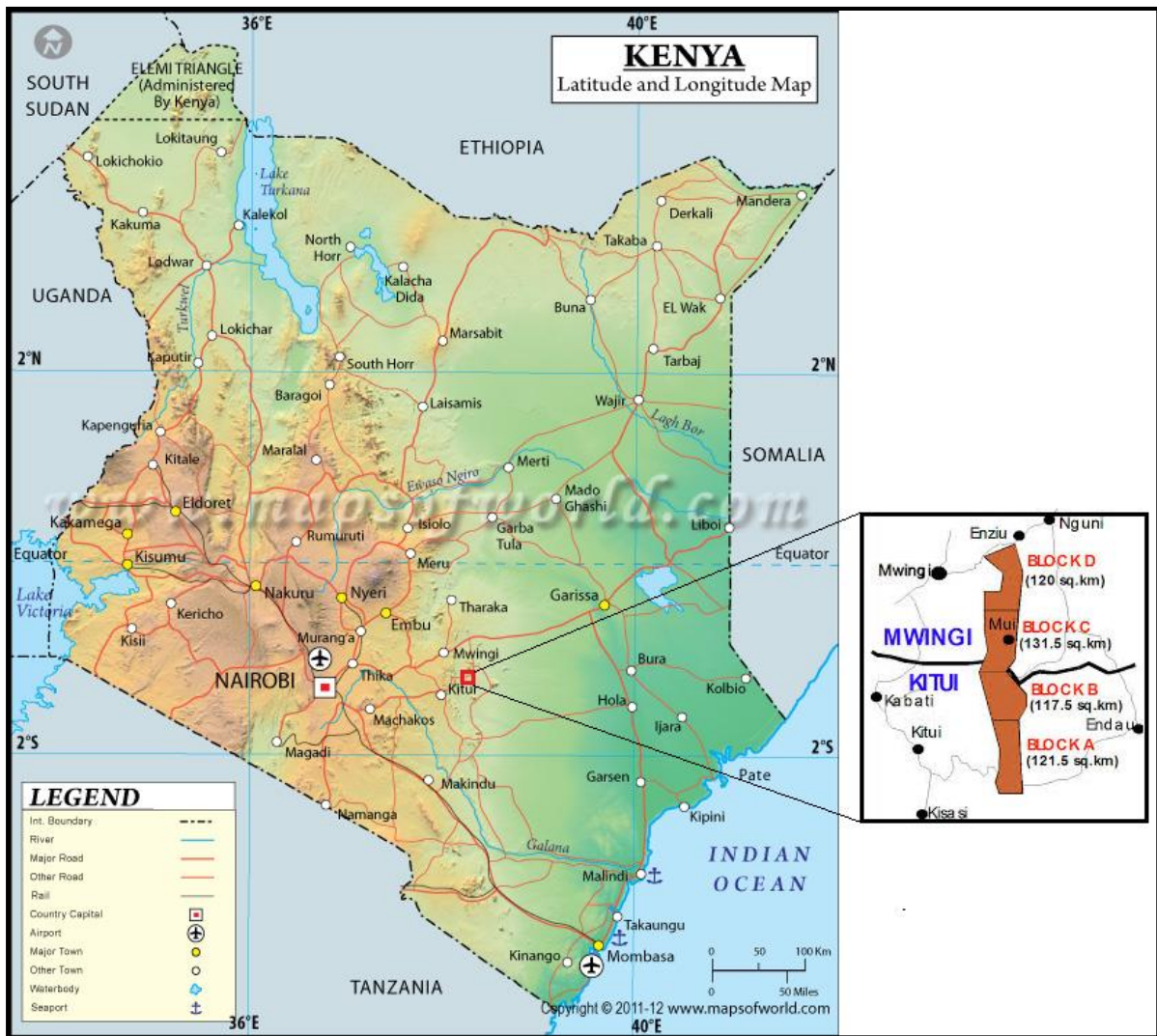
**Figure 1: A map of the Country, Kenya [17] and the coal blocks in Mui Basin in Kitui County, Kenya [18]**

## 2.2 Data

Two types of data were collected from National Centre for Environmental Prediction's (NCEP) Global Data Assimilation System (GDAS) archived meteorology data which is run 4-times a day i.e. (00, 06, 12 and 18 UTC) for Mui by use of longitude and latitude. NCEP post processing of the GDAS converts the data from spectral coefficient form to 1-degree latitude-longitude grids and from sigma level to mandatory pressure levels. However, the data is usually available in Air Resource Laboratory (ARL) server in GRIB format. The wind roses depict the frequency of occurrence of winds in each of the specified wind direction sectors, wind speed classes for a given location, and time period. Hysplit trajectories and dispersions for selected months were generated from archived data for Mui by use of longitude and latitude.

## 3. Methods

To answer the question on how coal mining will affected people health on the nearby communities, the methods outlined below were used.

### 3.1 Wind Rose Analysis

A wind rose gives a very succinct information-laden view of how wind speed and direction are typically distributed at a particular location and thus the distribution of air pollution plume located upwind of a given location. The wind roses shown here contain additional information, in that each spoke is broken down into discrete frequency categories that show the percentage of time that winds blow from a particular direction at certain speed ranges.

### 3.2 HYSPLIT Trajectory Analysis

A trajectory is the path that a single pollutant in air follows through space and is a function of time. At a minimum, Hysplit model requires U, V (the horizontal wind components), T (temperature), Z (height) or P (pressure) and the pressure at the surface, $P_o$. If wet deposition processes were to be included, then the model also requires the rainfall field. Normally ground level (<=10 m) winds are available from most meteorological models. However, if these winds speed are not provided, the estimates are made using a logarithmic wind profile for neutral conditions. In this study the Lagrangian particle model was used to compute trajectories of a large number of particles to describe the transport and diffusion of tracers in the atmosphere. The main advantage of Lagrangian models was that, unlike in Eulerian models, there is no numerical diffusion. A forward trajectory was run for two hours starting at 0000Z from the source. Vertical motion calculations were done by use of vertical velocity method.

### 3.3 Pollutant Dispersion Analysis

Pollution dispersion is the process of spreading out pollution emission over a large area and thus reducing their concentration. Wind speed and environmental lapse rates directly influence the dispersion pattern. In Gaussian models, the spread of a plume in vertical horizontal direction assumed to occur by simple diffusion along the direction of the mean wind. The maximum ground level concentration is calculated by means of the following Equation.

$$C_x = \frac{Q}{\pi \sigma_y \sigma_z u} e^{-1/2 \left[\frac{H}{\sigma_z}\right]^2} e^{-1/2 \left[\frac{y}{\sigma_y}\right]^2} \quad . (4)$$

Where; $C_x$ is the ground level concentration at some distance x downwind ($g/m^3$), **Q** the average emission rate (g/sec), **u** the mean wind speed (m/sec), **H** the effective stack height (m), $\sigma_y$ the standard deviation of wind direction in the horizontal (m), $\sigma_z$ the standard deviation of wind direction in the vertical (m), **y** the off-center line distance (m) and **e** is the natural log equal to 2.71828.

In this study, seasonal pollutant dispersions were plotted using archived meteorological data from HYSPLIT ready model. Dispersions plotted showed spreading out of pollution emission over a large area and thus reducing their concentration. Wind speed and environmental lapse rates directly influenced the dispersion pattern. In Gaussian models, the spread of a plume in vertical horizontal directions were assumed to occur by simple diffusion along the direction of the mean wind.

### 3.4 Generalized case

Finally, a wind power formula was used to determine wind speed at certain height above the ground surface and stability class.

$$U_z /U_g = (H_z/H_g)^n \quad . (5)$$

Where $U_z$ is wind velocity at height Z, $U_g$ is wind velocity at ground station, $H_z$ is height of Z above ground station, $H_g$ is ground station height (usually 10 m)and n= a function of Pasquill stability class and terrain type.

Wind speed was computed at a certain height say 20m above the ground surface and a stability class. Based on this for instance, a surface wind speed of about 3 ms$^{-1}$ was used to compute the time taken by a parcel of pollutant travelling at approximately 10 meters above the ground to a certain area. It was calculated using different stability classes as given by Pasquill [19].

Using the formula;
$$U_z/U_g= (h_z/h_g)^n \quad . (6)$$

Then,

$$U_z=U_g (h_z/h_g)^n \quad . (7)$$

It implies that;

$$U_z=3 \text{ ms}^{-1} (20 \text{ m}/10\text{m})^{0.15} = 3.32 \text{ ms}^{-1} . (8)$$

Using the formula Distance= Speed x Time
Hence Time= Distance/Speed

Therefore, a region say one kilometer from the mining site, the time taken by a pollutant picked at the site would be calculated as follows;

Time= 1000 m /3.32 ms$^{-1}$ =301.2 seconds (approximately 5 minutes)

This implied that the pollutant traveling at 10 m high with a speed of 3.32 ms$^{-1}$ would reach residents on the direction of prevailing wind after 5 minutes after it will be picked from the mining site. The time for regions beyond one kilometer would be calculated depending on the terrains and distance from the mining site.

The most highly prone people will be those working or living within a radius of one kilometer from the coal mining sites due to their proximity since they will receive the polluted air in less than 5 minutes and those residing between northwestern and northeastern sectors of the mining sites.

### 4. Results and Discussion
Results of wind rose, HYSPLIT pollutant trajectory and dispersion analysis obtained in this study are discussed according to the four distinct seasons of the year as follows:

### 4.1 Transport and dispersion condition in DJF
From the generated wind roses for the December-January-February (DJF) season it is evident that winds were mainly southerly and south easterly.

As may be seen from figure 1a below, LMN showing the wind rose diagrams for the month of December, southerly wind speeds varied between 1-3 ms$^{-1}$ and depicted a 56-70% frequency. South Easterlies also had similar magnitudes but with a 28-42% frequency. Calm winds were however notable in the month of January.

From the trajectory analysis carried out pollutants are depicted to be dispersed northwestward of the source during this season. Figure 2a shows the forward Hysplit pollutant trajectory during the month of December. NNW and NW trajectories are observed within 5km radius from the mining site and between 5km and 8km respectively. From dispersion analysis, pollutant concentration decreases outwards from the source during the same period as expected. The Hysplit pollutant dispersion for the month of December is as shown in figure 3a. From the figure a maximum concentration of 4.8E-04 $\mu gm^{-3}$ is observed at the source decreasing directly downwind to 1.0E-04 $\mu gm^{-3}$', 1.0E-05 $\mu gm^{-3}$ and 1.0E-06 $\mu gm^{-3}$ at 5km, 20km and beyond 20km respectively. Pollutant concentration is also observed to decrease relatively fast away from the center-line. The lowest pollutant concentration that can be observed during the month of December over the study region is 2.2E-11 $\mu gm^{-3}$.

## 4.2 Transport and dispersion condition in MAM

During this season the winds were generally southerly and southwesterly with much of the wind speeds ranging from 1-3 ms$^{-1}$. Figure 1b shows wind rose diagram for the month of April. As is evident in the figure southerly winds are shown to be dominant and depicting a 1-3 ms$^{-1}$ speed variation and with a 56-70% frequency. South Westerly winds on the other hand are calm with a 28-42% frequency.

During this season pollutants are depicted to be dispersed generally westward from the source. A forward Hysplit pollutant trajectory for the month of April is shown in figure 2b. As is evident from the figure, NW, W and WSW forward Hysplit trajectories can be observed within 3km circle centered at the mining site, between 3km and 7km and beyond 8km respectively. During MAM season pollutant concentration decreases from the source towards WSW from the dispersion analysis carried out. The Hysplit pollutant dispersion for the month of December is as shown in figure 3a. As is evident in the figure a maximum concentration of 4.7E-04 $\mu gm^{-3}$ is observed at the source decreasing directly downwind to 1.0E-04 $\mu gm^{-3}$, 1.0E-05 $\mu gm^{-3}$ and 1.0E-06 $\mu gm^{-3}$ at 5km, 20km and beyond 20km respectively. Pollutant concentration is also observed to decrease relatively fast away from the center-line as is the case during the DJF season. The lowest pollutant concentration that can be observed in April is 1.3E-11 $\mu gm^{-3}$.

## 4.3 Transport and dispersion condition in JJA

From the wind rose analysis carried out during this study, the June-July-August (JJA) seasonal average wind speed was noted to be less than 3 ms$^{-1}$ especially during the onset of the season i.e. in the month of June. From fig. 1c, wind speeds are also seen to be predominantly South Westerly with an average frequency of between 56-70%. The southerly winds are less frequent i.e. 28-56% even though both are of the same magnitudes.

From the trajectory analysis carried out pollutants are depicted to be dispersed generally northwestward from the source during this season. Figure 2c shows the forward Hysplit pollutant trajectory during the month of July. The figure depicts slightly NNW and NW trajectories within an 8km circle centered at the source and beyond 8km respectively.

As is the case with the other seasons, pollutant concentration decreases outwards from the source during the same period as expected. Figure 3c shows the Hysplit pollutant dispersion for the month of July. As may be observed in the figure, a maximum concentration of 3.6E-04 ugm$^{-3}$ is observed at the source decreasing directly downwind to 1.0E-04 $\mu$gm$^{-3}$, 1.0E-05 $\mu$gm$^{-3}$ and 1.0E-06 $\mu$gm$^{-3}$ at 5km, 20km and beyond 20km respectively. A slow decrease in pollutant concentration away from the center-line as compared to the DJF and MAM seasons is observed during this period. The lowest pollutant concentration that can be observed over Mui basin during the month of July is 6.1E-12 $\mu$gm$^{-3}$

### 4.4 Transport and dispersion condition in SON

During the SON season, southerly winds prevailed over the south easterlies. Generally the wind speeds during the same period were slightly <3 ms$^{-1}$. Figure 1c shows the wind rose diagrams for the area of study during the month of September. During this month Southerlies with wind speeds of between 1-3 ms$^{-1}$ were dominant with 84-100% frequency.

During the SON season a general northward Hysplit pollutant trajectory is observed in the study area. Figure 2d shows the forward Hysplit pollutant trajectory during the month of September.  As may be seen in the figure a NNW Hysplit pollutant trajectory is depicted from the source and beyond the 8km circle. Pollutant concentration decreases outwards from the source during the same period as is the case with the other seasons as expected although at a slightly faster rate. The Hysplit pollutant dispersion during the month September is as shown in figure 3d. A maximum concentration of 2.5E-04 $\mu$gm$^{-3}$ is observed at the source decreasing directly downwind to 1.0E-04$\mu$gm$^{-3}$, 1.0E-05 $\mu$gm$^{-3}$ and 1.0E-06 $\mu$gm$^{-3}$ at about 2km, between 2km and 10km and >10km respectively. A slow decrease in pollutant concentration away from the centerline as is the case during JJA is also observed during this period. The lowest pollutant concentration that can be observed over Mui basin during the month of September is 4.7E12 $\mu$gm$^{-3}$.
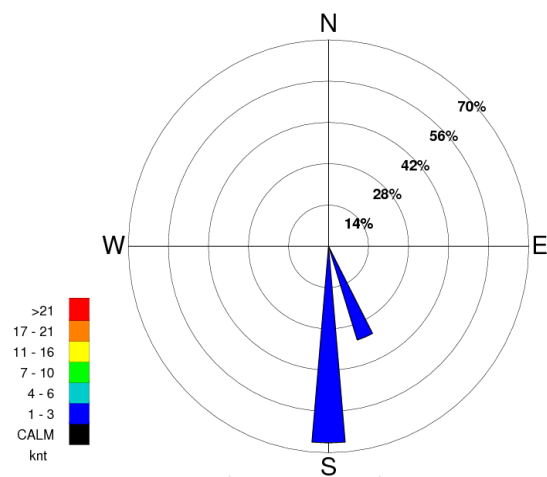


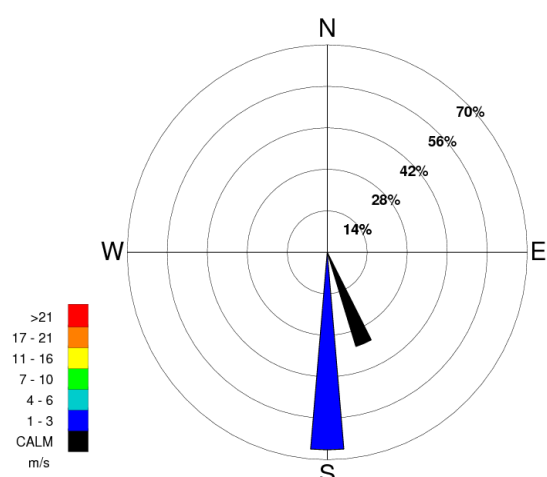**Figure 1a: Wind orientation of Mui basin for of December 2011**



**Figure1b: Wind orientation of Mui basin for the month April 2011**
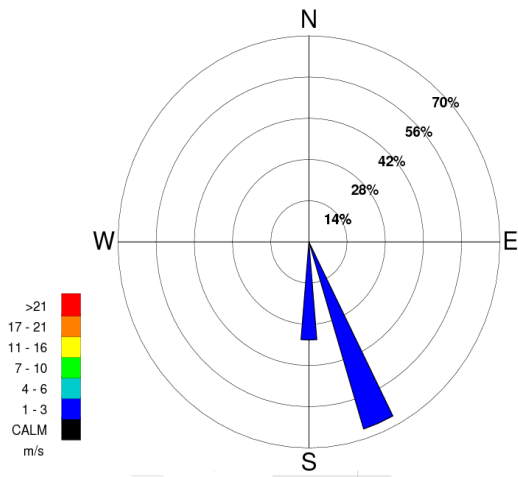
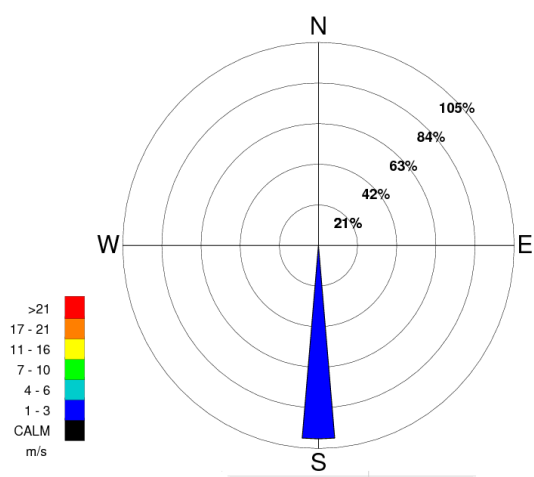**Figure 1c: Wind orientation of Mui basin for month of July 2011**

**Figure1d: Wind orientation of Mui basin for the month of September 2011**

**Source:** NOAA Air Resources Laboratory ready server. The wind rose calculation started at 00Z and ended at 06Z for latitude -1.37 and longitude 38.02
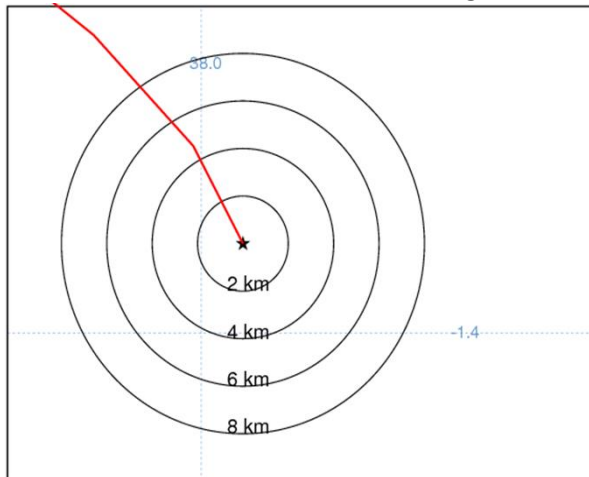


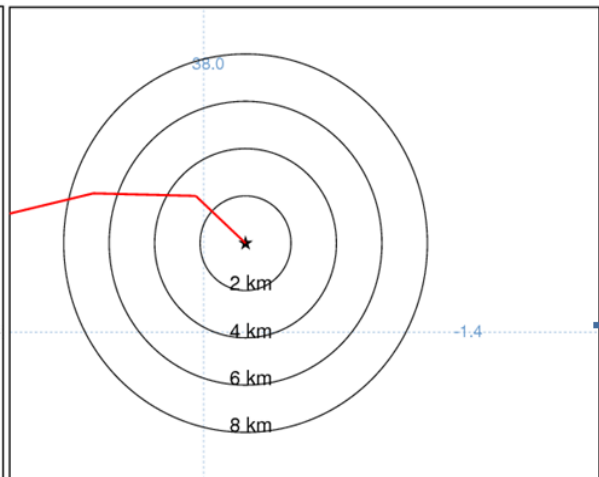**Figure 2a: Forward hysplit trajectory for the month of December**

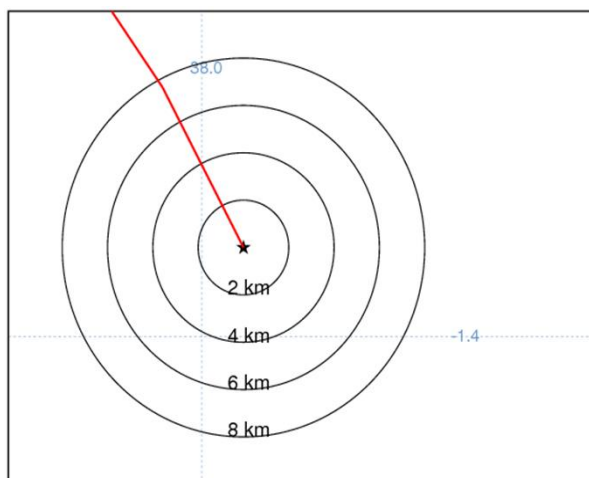**Figure 2b: Forward hysplit trajectory for the month of April**



**Figure 2c: Forward HYSPLIT trajectory for the month of July**
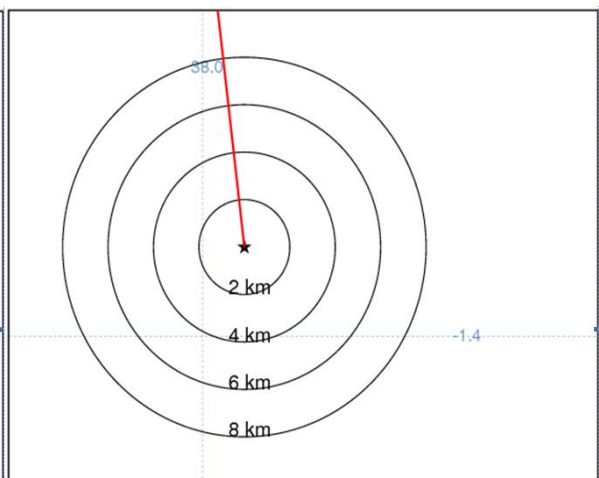
**Figure 2d: Forward HYSPLIT trajectory for the month of September**

**Source:** NOAA Air Resources Laboratory ready server starting at 06Z and run for 8hours.
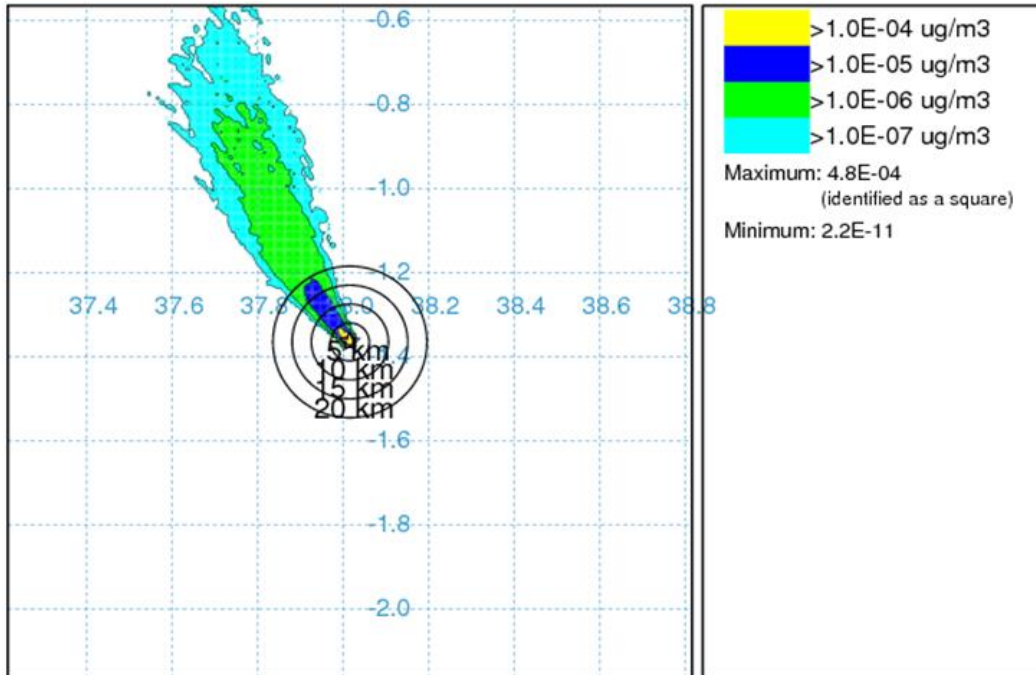

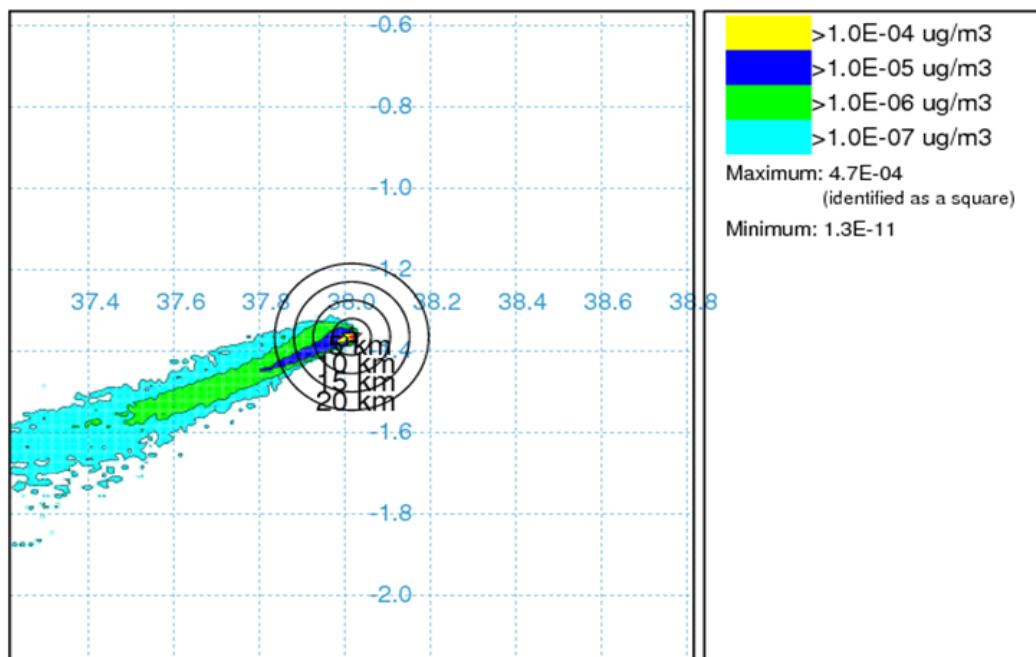
**Figure 3a: Hysplit dispersion for the month of December.**



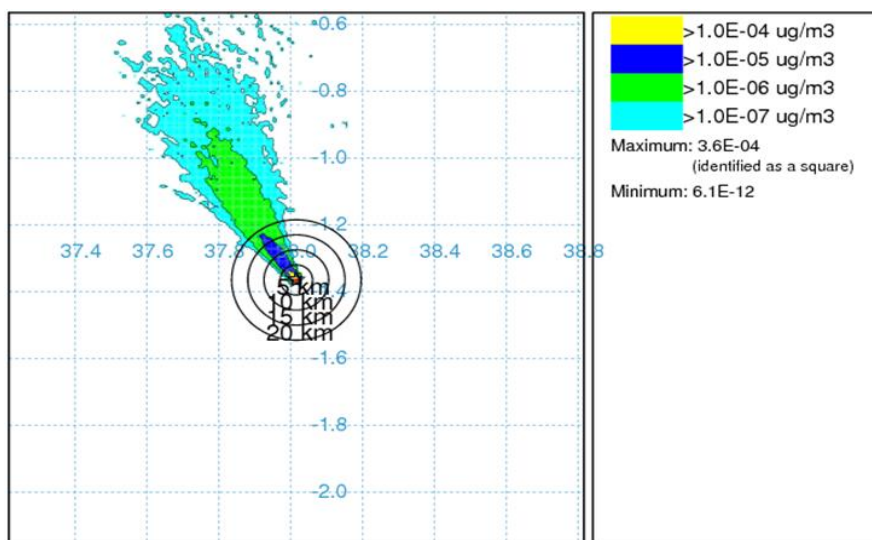**Figure 3b: Hysplit dispersion for the month of April.**
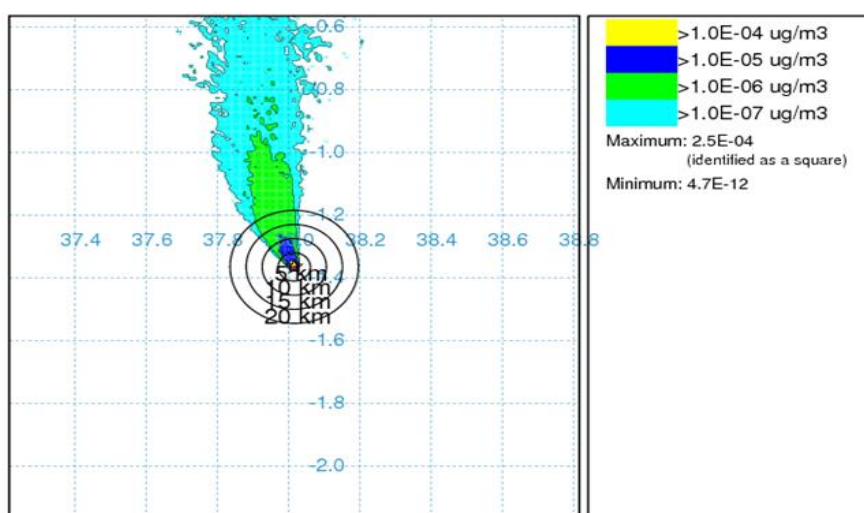
**Figure 3c: Hysplit dispersion for the month of July.**



**Figure 3d: Hysplit dispersion for the month of September.**

**Source:** NOAA Air Resources Laboratory ready server. Concentration in (μg/m³) averaged between 0m to 100m release started from 0600Z to 1400Z.

## 5. Conclusions

Wind rose analysis revealed that southerly and southeasterly winds are observed to be dominant over the study area throughout the year. However, during the month of December, winds were expected to be north easterlies owing to the position of the ITCZ in the southern hemisphere but due to the elevation of the study area, local forcing lead to enhanced southerly orientation of the wind patterns. Topography was considered a local forcing that significantly modified the large-scale temperature, moisture and wind flow patterns [20]. However, the ITCZ is diffuse close to the surface over land in East Africa owing to high terrain elevations but manifest itself clearly between 750mb and 700mb [21] hence no effect on wind flow patterns over the area of study. Due to the observed wind orientation and strength a generally north and northwestward trajectory of pollutants is depicted throughout the year over the study region through Hysplit trajectory analysis. This therefore implies that the residents to the north and northwest of the proposed coal mining area would be at high risk of the pollutants.

From the Hysplit dispersion analysis a source pollutant concentration of about 1.0E-04 µg/m$^3$ is dispersed generally northwestwards and decreases to about 1.0E-07 µg/m$^3$ at the end of dispersion run-time of 8 hours. The rate of dispersion was noted to be high within 5km from the source decreasing further away as shown in the figures. Though the highest maximum pollutant concentration was observed during the month of December, worst pollutant exposure would be experienced during the JJA season. The onset of this season experiences cool climatic conditions due to the blocking highs of Mascarene and St .Helena, which brings about the Quasi-stationary wave on the southern region hence temperature inversions and subsequently, this could lead to low-level concentration of pollution over this region of study hence worse scenario. Therefore those residing within and in the neighborhood of the mining site (less than 5km) would be highly exposed and subsequently affected by the pollutants from the source during this season. The people to the far north and western side of the proposed mining site would be less affected by the pollutants owing to high dilution of the pollutant. During the onset of the DJF season the winds are relatively strong and the pollutants will be dispersed further north and northwestwards. During both the MAM and SON seasons the pollutant concentration was moderate. However minimum effect is expected during SON due to stronger northerly winds compared to the calm conditions observed at the onset of the MAM season.

The study showed that there would be a potentially direct health threat exposed to the miners, residents of the study area due to the close proximity and those residing in the northwestern to northeastern sector of the proposed mining area since much of the winds were southerlies and sometimes calm. Hence this was clear evidence that those people will be affected negatively by the coal related illness.

## 6. Recommendations

Reviews of available information on air pollution suggest that there is lack of data on source emission and spatial distribution of air pollutants in coal mining areas. Therefore a systematic effort should be made to study the spatial and temporal distribution of air pollutants in the atmosphere and their dispersion which would not only identify air pollutants source but also to devise strategies to control air pollution. The study showed that there was negative potential impact to the people of Mui basin and the following should be done to ensure safety of the residents should coal mining take place in the basin.

- Further investigations on the content of the volatile matter should be carried out to ascertain the exact constituents and the amount likely to harm human beings.

- There should be proper planning of residential houses away from the mining sites and relocation of those living between northeastern and northwestern sector of the proposed mining site.

- Hospitals with good facilities should be set up so that the residents would access them with ease for regular medical check up on possible diseases arising from these pollutants,

- Discharging of the waste on an unstable or permeable ground could pollute ground water resources in the mining area, for instance, when the ground collapses or content seeps to the water flow system, a research should be carried out to investigate the potential impact of this mining activity on the water resources to the residents of Mui and its environs.

The assessment was based on the wind climatology of the mining area and therefore mainly qualitative. Quantitative impacts assessment can only be done if the pollutants from the mining operations are identified and emission rates determined. The paper therefore provides baseline information that can be used to support decision making in planning to reduce potential impacts of air pollutants on human health.

## References

[1] Ndolo, J.M. (2004) Coal exploration monthly report, Ministry of Energy, Kenya.

[2] Muthama, N. J. (1989) Total Atmospheric Ozone Characteristics over a Tropical Region, MSc. thesis, University of Nairobi, September 1989.

[3] Burt, E., Orris, P. & Buchanan, S. (2013) Scientific evidence of health effects from coal use in energy generation. *Chicago and Washington: School of Public Health, University of Illinois and Health Care Without Harm.*

[4] Callen, M.S., de la Cruz, M.T., Lopez, J.M., Navarro, M.V. & Mastral, A. M. (2009) Comparison of receptor models for source apportionment of the $PM_{10}$ in Zaragoza (Spain). *Chemosphere*, **76:** 1120-1129.

[5] Prieditis, H. & Adamson, I.Y.R. (2002) Comparative pulmonary toxicity of various soluble metals found in urban particulate dusts. *Experimental Lung Research*, **28:** 563-576.

[6] Magas, O.K., Gunter, J.T. & Regens, J.L. (2007) Ambient air pollution and daily pediatric hospitalizations for asthma. En*vironmental Science and Pollution Research*, **14:** 19-23.

[7] Wild, P., Bourgkard, E. & Paris, C. (2009) Lung cancer and exposure to metals: The epidemiological evidence. *Method Molecular Biology,* **472:** 139–167.

[8] Adler, R. & Rascher, J. (2007) A Strategy for the management of acid mine drainage from gold mines in Gauteng. Report. No. CSIR/NRE/PW/ER/2007/0053/C (Pretoria: Council for Science and Industrial Research).

[9] GoK/MoE (2002) Mui Basin coal exploration progress report. Government of Kenya, Ministry of Energy Headquarters in Nairobi.

[10] GoK/MoE (2011) Coal potential and investment opportunities in Kenya. Government of Kenya, Ministry of Energy monthly pamphlet, October 2011.

[11] GoK (2002) National development plan 2002-2008, Nairobi, Government of Kenya (GoK).

[12] KPLC (2006) Annual report, 2006, Nairobi, Kenya Power and Lighting Company.

[13] AFREPREN (2005) Occasional Paper 26: Renewables in Kenya's electricity industry: A review of geothermal and cogeneration technologies, Nairobi. (AFREPREN).

[14] AFREPREN (2006). The potential contribution of non-electrical renewable energy technology (RETs) in poverty alleviation in Eastern Africa: The case of wind pumps, ram pumps, and treadle pumps in Kenya and Tanzania, Nairobi, African Energy Policy Research Network (AFREPREN).

[15] Balla, P. (2005) The potential contribution of non-electrical renewable energy technologies (RETs) towards poverty alleviation: Non-electrical water pumping technologies for irrigation, Nairobi, energy, environment and development network for Africa.

[16] Mukabana, J. (2009) Climate of eastern province, Meteorological department, Report No. **65**, pp 50-60.

[17] MapXL, Inc., Kenya Latitude and Longitude Map. Maps of World. US Office http://www.mapsofworld.com/lat_long/kenya-lat-long.html#. (Accessed on 10th July, 2015)

[18] Patrick M. (2015) A Map of the Coal Blocks in Mui Basin in Kitui County, Kenya. Africa Eco News. http://www.africaeconews.com/how-the-call-to-divest-from-fossil-fuel-is-rattling-the-african-continent/

[19] Pasquill, F. (1961) The estimation of dispersion of windborne material. *Meteor. Mag.*, **90**(1063): 33-49.

[20] Mukabana, J. R. & Piekle, R. A. (1996) Investigating the influence of synoptic-scale monsoonal winds and mesoscale circulations on diurnal weather patterns over Kenya using a mesoscale numerical model. *Monthly Weather Review,* **124**(2): 224-244.

[21] Kiagi, P. M. R., Kavishe, M. M. & Patnaik, J. K. (1981) Some aspects of the mean tropospheric motion filed in east africa during the long rains season. *Kenya Science and Technology Series*, **A2:** 91-103.